Peer-reviewed version available at Polymers 2018, 10, 1304; doi:10.3390/polym10121304

Article

Fabrication and characterization of flexible medical-grade TPU filament for Fused Deposition Modeling 3DP technology

Agnieszka Haryńska [1], Iga Gubańska [1], Justyna Kucińska-Lipka [1,*] and Helena Janik[1]

[1] Gdansk University of Technology, Chemical Faculty, Polymer Technology Department, Narutowicza Street 11/12, Gdansk 80-232

* Correspondence: juskucin@pg.edu.pl ; Tel.: + 48 (58) 347-12-14

Abstract: The possibility of using additive manufacturing (AM) in the medicine area has created a new opportunities in health care. This has contributed to a sharp increase in demand for 3D printers, their systems and materials that are adapted to strict medical requirements. We described herein a medical-grade thermoplastic polyurethane (S-TPU), which was developed and then formed into a filament for Fused Deposition Modeling (FDM) 3D printers during a melt-extrusion process. S-TPU consisting of aliphatic hexamethylene 1,6-diisocyanate (HDI), amorphous α,ω-dihydroxy(ethylene-butylene adipate) (PEBA) and 1,4 butandiol (BDO) as a chain extender, was synthesized without the use of a catalyst. The filament properties were characterized by rheological, mechanical, physico-chemical and in vitro biological properties. The tests showed biocompatibility of the obtained filament as well as revealed no significant effect of the filament formation process on its properties. This study may contribute to expanding the range of medical-grade flexible filaments for standard low-budget FDM printers.

Keywords: medical-grade filament; thermoplastic polyurethane; fused deposition modeling; filament forming; 3D printing

Graphical Abstract:

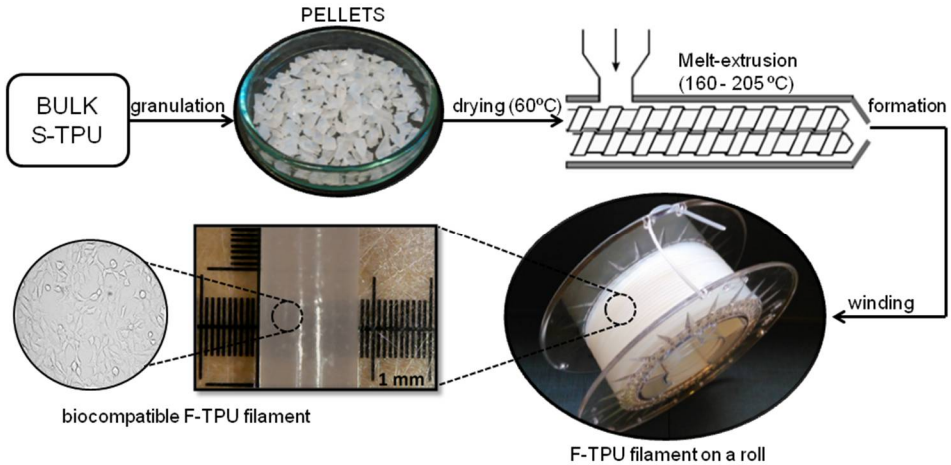

1. Introduction

Additive manufacturing (AM) technologies have become a very effective and powerful tool in the health care industry [1–3]. Three-dimensional printers (3DP) are no longer the only rapid prototyping devices. The practical applications of an AM technology in medicine are more and more frequent. The use of 3D printers in combination with tools, such as computer-aided design (CAD) and radiographic methods (CT scans, MRI or X-rays), allow producing customized implants [4–6], or precise anatomical models for surgical planning [7,8]. Medical products fabricated via 3DP may

Peer-reviewed version available at Polymers 2018, 10, 1304; doi:10.3390/polym10121304

be divided into five broad categories, i.e. surgical training systems (artificial organs, anatomical models), patient-matched devices (implants and prosthesis), tissue engineering constructs (scaffolds), pharmaceutical systems (drug delivery), as well reproduced tissues and organs. However, these medical products are characterized by different requirements and properties which are associated with the selection of proper material and a 3D printing technology. For example, reproduced temporal bones for drilling surgery training as well as artificial organs for a teaching purpose or preoperative planning should primarily exhibit high dimensional accuracy and organoleptic properties, e.g. texture, tactile sensation and viscoelasticity, which must imitate their biological counterparts [8,9]. Thus, 3D printed medical devices provide enormous assistance for surgeons and medical students. Moreover, tissue scaffolds, which have to provide physical support for new growing tissues and promote tissue regeneration, primarily should be highly biocompatible and degradable within a given timeframe. They should also have a three-dimensional, highly porous structure, and exhibit appropriate mechanical properties similar to the regenerated tissues [10,11]. These strict medical requirements limit the possibility of using conventional 3D printing materials or systems. Therefore, there is a need to look for and develop more advanced solutions and materials. AM technologies differ in operational principles, used equipment and materials. It is worth mentioning that, according to ASTM F2792-10 [12], AM is the official term but 3D printing (3DP) is a common definition of the family of AM technologies. Several widely used 3D printing technologies in medicine are: selective laser sintering (SLS), PolyJet (PJ), stereolithography (SLA) and fused deposition modeling (FDM) [13]. Bioprinting is a separate branch of AM technologies. A bioprinting process consists in depositing drop by drop materials known as "bioinks" to reproduce functional tissues/organs or create bioactive tissue scaffolds. A bioink mostly consists of isolated living steam cells, nutrients and/or a matrix based on hydrogel biomaterials [14,15]. However, these innovative solutions require highly advanced machinery, equipment and materials, which are used by collaborating specialists in material engineering, biotechnology and surgery. This results in huge and expensive operation and high production costs of 3D printed medical products. A possible solution is the use of the FDM method. FDM is one of the most cost-effective 3DP technologies, both in terms of purchase and service. According to Oskuti et. al, objects printed with the use of FDM are significantly less toxic than SLA-printed parts for living organisms[16]. FDM has already been successfully used for printing biomedical devices [17,18]. Additionally, a fast-growing open-source community provides access to expert solutions and knowledge in the use of FDM 3DPs, which further reduces costs and facilitates the use of these devices. FDM is based on the layered deposition of plasticized polymeric material on a movable platform. The polymeric material in the form of a filament is fed to the miniature temperature-controlled extruder, where the plasticization takes place. Filament is a thin wire with a strictly defined diameter. One of the filament formation methods is a melt extrusion process [19]. There is a variety of commercially available filament types that exhibit a wide range of properties, however, medical-grade filaments market is still developing. One of the few companies supplying certificated medical-grade filaments dedicated for FDM 3DP is Poly-Med (USA). Their series of filaments (Lactoprene® 100M, Caproprene® 100M, Max-Prene® 955, Dioxaprene® 100M), have been recently examined by Mohseni et al. [20] as a potential materials for tissue engineering 3D constructs. The mentioned filaments based on polylactide (PLA), polycaprolactone (PCL), poly(lactic-co-glicolic acid) (PLGA), and polydioxanone (PDO). Whereas, Bioflex® supplied by FiloAlfa (Italy) is a highly durable and flexible filament, belonging to the group of so-called thermoplastic elastomers (TPE). Its medical properties are confirmed by USP Class VI and ISO 10993-4/5/10 (cytotoxicity, hemolysis, intracutaneous and injection tests). However, degradation studies performed by our team showed that this material is highly resistant to acidic and alkaline environments **(supplementary data 1).** This significantly limits its use, for example in tissue engineering constructs, in which the material should degrade and resorb proportionally to the rate of tissue growth [21]. Currently, the most commonly used "medical" filaments for FDM 3D printers are thermoplastic biopolymers based on crystalline PLA or PCL. They provide satisfactory properties required for medical devices and structures such as biodegradability, bioresorbability and adequate/suitable durability [22–24]. However, there is lack of

Peer-reviewed version available at Polymers 2018, 10, 1304; doi:10.3390/polym10121304

filaments available on the market, which provides properties (texture, flexibility, tactile sensation) that allow for native tissues or organs mimic. These are important requirements in case of appropriate surgical training systems production via 3DP technology for the surgeons and medical students [9]. Materials that may be alternative to medical filaments based on PCL and PLA are properly designed thermoplastic polyurethanes (TPUs). According to the literature, they exhibit biocompatibility and hemocompatibility [25]. Moreover, TPU degradation rate can be controlled as well [26]. Biostable TPUs are widely known and used in medicine as prosthetics, implants, artificial blood vessels, or gene carriers [27]. What is more, the TPUs have been already successfully applied as tissue engineered scaffold [28] nerve guidance channels [29], breast implants, dialysis membranes or aortic grafts [30]. Additionally, we have not recorded certified medical-grade TPU filaments available on the market. Whereas, studies performed by Jung et al. [31] and Tsai et al. [32] confirm the legitimacy of using appropriately designed TPUs (based on aromatic polyether urethane and Tecoflex®, respectively) as filaments to fabricate advanced structures for tissue engineering purpose via FDM. Looking for new flexible medical-grade materials for filament fabrication may contribute to the popularization of low-budget FDM printers as a cost-effective tool in health care.

Based on these premises, in this paper, we report our studies on novel flexible and medical-grade filament (F-TPU), dedicated for FDM 3D printing technology. For this purpose, we have synthesized TPU using raw materials suitable for the synthesis of biomedical polyurethanes [33] like aliphatic hexamethylene 1,6-diisocyanate (HDI), amorphous α,ω-dihydroxy(ethylene-butylene adipate) (PEBA) and 1,4 butandiol (BDO) as a chain extender. Discussable subject in terms of polyurethane synthesis is application of organotin catalysts like dibutyltin dilaurate (DBTDL) and stannous octoate ($Sn(Oct)_2$) [34,35]. To avoid possible accumulation of these catalyst in TPU matrix, which may affect the deterioration of biocompatibility and hemocompatibility of the material [36], we did not apply it in the synthesis of TPU described in this paper.

This study is divided in two main sections; the first section focus on the synthesis in bulk and characterization of cast polyurethane (S-TPU) and filament fabrication (F-TPU) via melt-extrusion. The second part is devoted to impact assessment of the filament forming process on selected physico-chemical and *in-vitro* biological properties. S-TPU was processed in filament (1,75 mm diameter) via melt-extrusion process. Then, physico-mechanical, chemical and rheological properties (tensile test, hardness, FTIR, contact angle, melt flow rate (MFR)), were characterized. Finally, a series of preliminary biomedical studies, such as hemocompatibility and cytotoxicity tests (NIH 3T3 cells) were performed for both materials S-TPU and F-TPU in order to assess the influence of the processing procedure on their properties.

2. Experimental

2.1. S-TPU synthesis

S-TPU was synthesized by standard two-step polymerization procedure (Figure 1) [25]. It was derived from amorphous PEBA (in contrary to PUR synthesized by using crystalline oligodiols [37,38]), aliphatic HDI and BDO chain extender. No catalysts were used in this synthesis (to avoid possible negative impact of the catalyst on the biocompatibility of the S-TPU [38,39]). In the first step prepolymerization reaction (8 wt% of free isocyanate groups) was carried out at 90°C for 6 hrs under vacuum by using PEBA and HDI. The reaction progress between PEBA and HDI over time was studied by the content of free isocyanate groups (F_{NCO} index) present in the prepolymer.

Preprints (www.preprints.org) | NOT PEER-REVIEWED | Posted: 24 October 2018 doi:10.20944/preprints201810.0552.v1

Peer-reviewed version available at Polymers 2018, 10, 1304; doi:10.3390/polym10121304

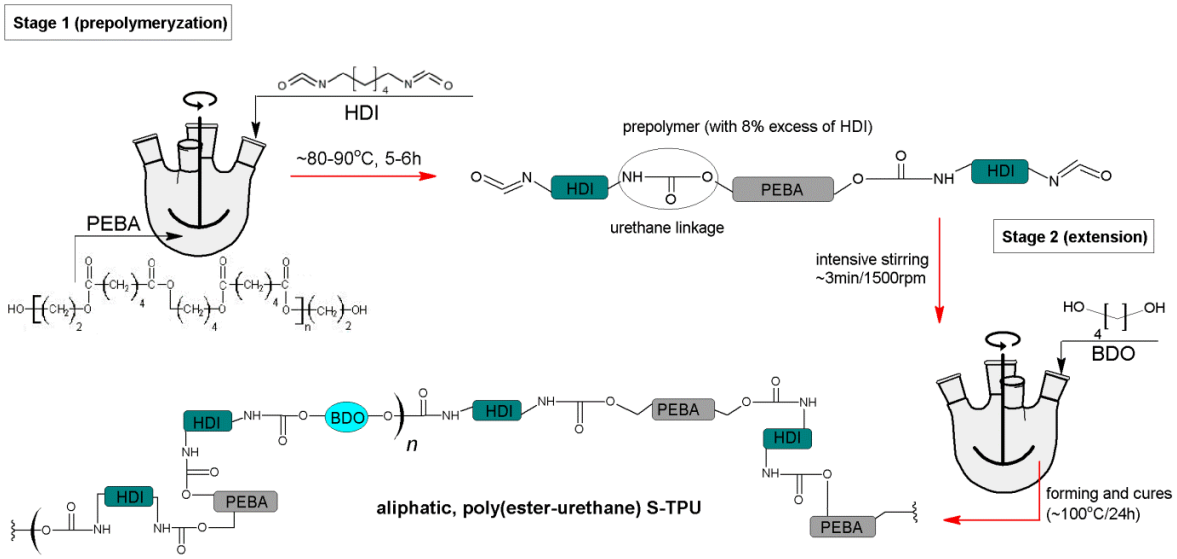

Figure 1. S-TPU synthesis scheme.

In the second step the BDO was added to the reaction mixture in the molar ratio of NCO:OH equal to 1,1:1. After 3 min of intensive stirring mixture was transferred into a mould, set at 80°C, for 3 hrs. Finally, the samples were left in a heating furnace at 100°C for 48 hrs to complete the reaction. The detailed characteristic of used raw materials was given in Table 1.

Table 1. Characteristic and chemical structure of used raw materials for the S-TPUs synthesis.

Compound	Supplier	Description	Structure formula
BDO	Brenntag, Germany	Low molecular chain extender, Mol mass = 88 g/mol, Physical state – clear liquid, Purity >95,5%, Tm = 204 °C, Boiling point ~ 230°C, ϱ(20°C) = 1,020 g/cm³	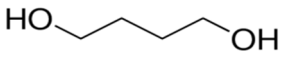
HDI	Sigma-Aldrich, Germany	Aliphatic diisocyanate, colorless liquid. Boiling point = 255°C, Flash point = 130°C, ϱ(25°C) = 1,05 g/cm³, Purity >99%, Tm = -67°C, Soluble in water, LD50 (rat)= 746 mg/kg.	
PEBA (POLIOS 55/20)	Purinova, Poland	Ester-based polyol, Mol mass = 2000 g/mol, Hydroxyl number = 54-58, Acid number – max. 0,6.	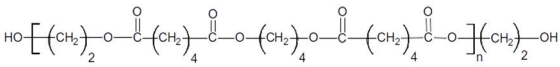

2.2. Identification of free isocyanate groups.

The determination of free isocyanate groups (F_{NCO}, %) was performed according to the PN-EN 1242:2006 standard. The percentage of free isocyanate groups was calculated by the formula (1);

$$\%NCO = \frac{(V_0 - V_1)*0,4}{m} \quad (1)$$

% NCO - percentage of unbound isocyanate groups [% mass]
V_0 - volume of HCl solution used for blank probe titration [cm³]
V_1 - volume of HCl solution used for the test sample titration [cm³]
m – sample mass [g]

2.3. Melt-extrusion of F-TPU filament.

Double-screw extruder IQLINE (EHP 2x20 IQ), Zamak Mercator Sp. z o.o. with nine heating zones, was used to obtain F-TPU filament. The custom-made molding nozzle diameter was equal to 1,5 mm and L/D screw ratio was 22. Several parameter combinations were tested in order to obtain F-TPU filament of stable diameter dimension. Filament diameter was controlled by an electronic caliper.

2.4. *Material characterization techniques.*

Density

Six S-TPU samples, of the 1cm^2 area, were weighed with accuracy to 0,0001g and then transferred to the analytical balance adjusted to density measurements (RADWAG AS 310/X). Density was calculated in comparison to distilled water (1,0 g/cm^3) at 20°C.

Melt flow rate (MFR)

S-TPUs MFR determination was carried out by using a load plastometer (ZWICK / Roell) according to the PN-EN ISO 1133-1:2011 standard. The value of MFR is expressed as a 1g of material extruded through the standard capillary (2,075 mm diameter) placed in a heating nozzle during 10 min [g/10min]. The S-TPU granules used in this study weighted 5g/measurement. The conditions to perform MFR study for S-TPUs were as follows: 180°C and 5 kg. Three repetitions were performed and the results were an average.

Mechanical characterization

Tensile strength and elongation at break were studied by using the universal testing machine Zwick & Roell Z020 according to PN-EN ISO 527-2:2012 with a crosshead speed of 500 mm/min and initial force of 1N. Five samples were studied and the results are an average. Hardness was measured by using Shore method according to PN-EN ISO 868:2005 standard. Obtained data were presented with Shore D degree (°Sh D). The results were an average of ten measurements.

Fourier Transform Infrared Spectroscopy (FTIR)

The FTIR analysis was performed with the use of Nicolet 8700 Spectrometer in the spectral range from 4000 to 500 cm^{-1} averaging 256 scans with a resolution of 4 cm^{-1}. The measurement was carried out both for the synthesized S-TPU and filament F-TPU.

Optical microscopy (OM)

The surface of solid S-TPU and filament F-TPU was studied via reflecting microscope. Samples were gold coated in the sputter coater Quorum 150T E. OM was performed at x800 magnification.

Contact angle (CA)

The CA of the solid S-TPU and filament F-TPU surfaces were determined at room temperature by using a Kruss Goniometer G10 (KRÜSS GmbH, Hamburg, Germany) with drop shape analysis software. A droplet of 2µL volume was deposited on the samples surfaces and images were taken at the static conditions using video instrument – drop shape analysis software DSA4. The results are an average of five measurement points of randomly selected at the samples' surface.

2.5. *Biological characterization.*

Short-term hemocompatibility test

Peer-reviewed version available at Polymers 2018, 10, 1304; doi:10.3390/polym10121304

Hemocompatibility was examined in Medical Academy Clinical Centre in Gdansk by using SYSMEX XS – 1000i analyzer. Sample of venous blood, from a healthy women, was used in this study. Biologic material, directly after being taken, was put into the sterile test-tube containing potassium acetate (factor which prevents blood clotting). Next step was to obtain the reference parameters for blood morphology. Then, both for, synthesized solid S-TPU and formed into filament F-TPU samples of 8 cm^2 with 8 ml of blood was added to the sterile test-tubes. The samples before hemocompatibility test were sterilized with argon gas plasma generated over H_2O_2. The samples were incubated in blood for 15 minutes at room temperature. After this time they were removed and blood was hematologically analyzed again. The results are an average of six measurements.

Indirect cytotoxicity test

Cell Culture Mouse embryonic fibroblast NIH 3T3 cells were cultured in High Glucose Dulbecco's modified Eagle's medium (DMEM HG, Sigma Aldrich, Poznan, Poland) supplemented with 10% fetal bovine serum (FBS) and antibiotics (100 µg/mL each of penicillin and streptomycin) at 37°C in a humidified atmosphere containing 5% CO_2. The effect of indirect MTT Proliferation Assay of S-TPU or F-TPU exposure on NIH 3T3 cell proliferation was determined by 3-(4,5-dimethylthiazol-2-yl)-2,5-diphenyl tetrazolium bromide (MTT) colorimetric assay using 100% concentrations of samples extract. Briefly, samples were initially sterilized in 70% ethanol for 30 min and then exposed to UV for 1 h for each side. MPTL samples were subsequently incubated in DMEM HG supplemented with 10% FBS and penicillin/streptomycin for 24 hrs at 37°C. The ratio of the total mass of the sample (S-TPU or F-TPU) to the volume of extraction medium was 100 mg/mL. After 24 h, extraction medium was collected, filtered through 0.2-µM filter and used to prepare 100% concentrations of S-TPU or F-TPU extract. NIH 3T3 cells (2 × 104) were seeded in 24-well plates for 24 h to allow for attachment and then, cell culture medium was replaced with S-TPU or F-TPU extracts for next 24 h, 48 h and 72 h. DMEM HG supplemented with FBS and antibiotics were used as a non-toxic control. At the end of exposure, 200 µL of MTT solution (4 mg/mL) was added and cells were incubated for 3 h at 37ºC. Next, culture medium was removed and water-insoluble formazan crystals were dissolved in dimethylsulfoxide (DMSO, Sigma Aldrich) and optical density of resulting solutions was measured at 570 nm using iMark Microplate Absorbance Reader (Bio-Rad, Warsaw, Poland). Results were presented as the percentage of cells proliferating after extract exposure relative to control cells cultured in extract-free medium. Obtained data are a mean of two separate experiments wherein each treatment condition was repeated in two wells.

Statistical Analysis

The results are average of two experiments, where each extract was tested twice. One-way ANOVA test followed by Bonferroni test for each comparison was performed using GraphPad Prism 6 software (GraphPad Software Inc., San Diago, CA, USA). p values of less than 0.05 were considered as significant (* $p < 0.05$; ** $p < 0.01$; *** $p < 0.001$; **** $p < 0.0001$; ns non-significant).

Analysis Cells Morphology

NIH 3T3 cells (2 × 104) were seeded in 24-well plates for 24 h to allow for attachment and then treated with S-TPU or F-TPU extracts for next 24 h and 72 h as described above. After exposure, cellular morphology was examined directly from the 24-well plate under Zeiss inverted microscope equipped with AxioCam digital camera (Zeiss, Göttingen, Germany).

3. Results and discussions

3.1. S-TPU synthesis – identification of free isocyanate groups

The reaction progress between PEBA and HDI over time was presented in Figure 2. After first hour of the prepolymer synthesis, FNCO index sharply decreased from 11 % to ~8%. After the next 4-5

hours, the F_{NCO} index has stabilized at the level of ~8 %, which indicated completion of the reaction between PEBA and HDI reagents. Thus, it can be concluded that PEBA and HDI reacts in a predictable and repeatable way what is significant aspect for further applications of these materials in biomedical field.

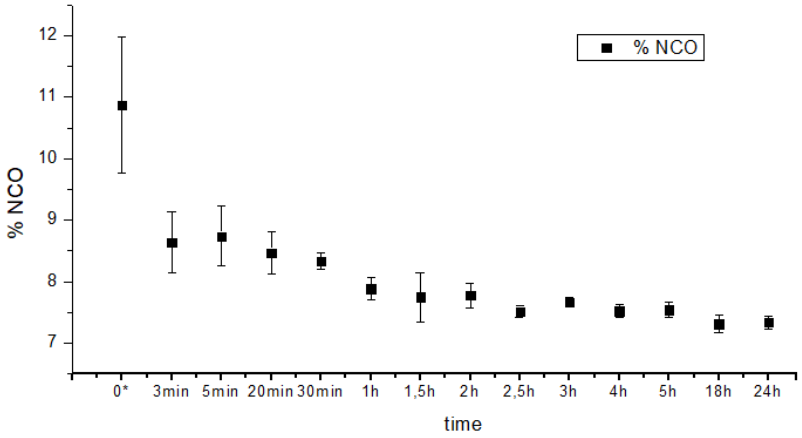

Figure 2. The changes of the isocyanate groups content (F_{NCO}, %) over reaction time between PEBA and HDI (prepolymerization step); * time "0" is related to the moment when the PEBA and HDI were mixed together in a whole volume of the reactive mixture.

3.2. Fabrication of F-TPU filament from synthesized S-TPU granules.

In Table 2 were presented selected melt-extrusion parameters used to fabricate the F-TPU filament, from S-TPU granules. It can be seen that operating parameters are closely related to the temperature profile of S-TPU extrusion. During process 1 and 2 (Table 2), very high head pressure and machine load, were noted. When the temperature profile was increased up to 210°C, the head pressure and machine load dropped significantly, to about 17 bar and 15-18%, respectively. The further increase of temperature profile (above 215°C) caused sharp decrease of head pressure (process 4, Table 2). This might be related to the viscosity of melt polymer. High melt viscosity hinder the free flow of polymer thought the narrow forming die. Therefore, in process 1 and 2 (Table 2) the temperature profile was not high enough to ensure free flow of polymer. Additionally in case of process 1 and 2, was observed an enormous swelling of the polymer at the die exit (Barus effect). During process 4 (Table 2) the polymer was undergoing degradation.

In the process of a filament forming via melt-extrusion process, it is necessary to maintain a constant value of head pressure. In other way, it is not possible to obtain an extrudate with a stable dimension. The combination of parameters in process 3* provided an appropriate profile which allow to obtain stable F-TPU filament with a constant diameter dimension (Table 2 – highlighted).

Peer-reviewed version available at Polymers 2018, 10, 1304; doi:10.3390/polym10121304

Table 2. Process parameters of F-TPU filament fabrication.

Lp.	ZONES TEMPERATURE PROFILE [°C]											OPERATING PARAMETERS		
	I	II	III	IV	V	VI	VII	VIII	IX	COUPLER	HEAD	ROTATION SPEED [rpm]	HEAD PRESSURE [bar]	LOAD [%]
1	160	165	170	175	185	185	190	195	190	190	185	20	37-48	45-50
2	170	175	175	180	190	200	205	200	200	195	195	20	28-30	20-28
3*	**170**	**175**	**180**	**190**	**200**	**205**	**210**	**210**	**205**	**200**	**200**	**20**	**17-18**	**15-18**
4	170	175	180	190	195	205	210	213	217	215	210	20	3-6	5-7

* Melt-extrusion profile that provide a dimensionally stable F-TPU filament.

3.3. Physico-mechanical properties of synthesized S-TPU.

Density of obtained S-TPUs were equal to 1,17 g/cm^3 what is similar to the references, which reports typical PUR density in the range of 0,2 – 1,2 g/cm^3 [40]. MFR is an important parameter of polymers processing allowing for an assessment of using thermoplastic materials for further technological procedure. The MFR value is directly related to the melt viscosity at the test temperature as well with the test load. With the increase of sample viscosity, the flow rate decrease. Thermoplastic materials designed for injection molding are characterized by very high MFR value (very high flow-rate and low melt viscosity), in contrast to thermoplasts intended for extrusion. In the FDM process, the material in the form of a filament is plasticized in a mini-extruder and passing through a heated nozzle with a diameter in the range of 0,3 – 0,8 mm, and settle down at movable platform. This is associated with a very short duration of heating and plasticizing of material. Therefore, the printed material should be relatively quick and easy to plasticize while maintaining the proper solidification rate, so that it will not flow from the layers built on the printer platform [41]. On the other hand, the strength and quality of the bonds formed between adjacent fibers depends on the growth of the neck formed among them and on the molar diffusion and randomization of the used polymeric filament across the interface [42,43]. Consequently, the degree of flow rate under FDM printing conditions should not be too high and sufficient/adequate for free flow of filament out of the nozzle. Additionally, it should be added that higher MFR value allows for higher print speed. Thus, at temperature of 200°C and test load of 5 kg the MFR value of S-TPU was 40,74±3,16 g/10 min, which might provide free flow rate of the printed material.

Tensile strength of injection-molded S-TPU samples was 26±2MPa, which was close to values determined for commercially available medical-grade PURs, like Carbothane® (39-67 MPa) and Desmopan® (25-50 MPa) [44–48], as well in the range of elastic TPU filament NinjaFlex® (26 MPa) [49]. Noted elongation at break of obtained S-TPUs was of 706±29 % and higher than Tecoflex® (365±25 % - 400±38 % [50,51], the medical-grade PUR for biomedical applications and NinjaFlex® filament (660%) [49]. Hardness of obtained S-TPUs was of 37,07±0,80°ShD and was comparable to the hardness of medical-grade TPU filament Bioflex® (27°ShD) [52]. It should be noted that as the filament hardness decreases, the difficulty of printing increases. This is particularly related to the folding of the filament on extruder rollers during printing process. Mechanical properties of S-TPU correspond to those PURs obtained with the use of organotin catalyst, dibutyltin dilaurate (DBTDL), described in our previous paper [53].

Peer-reviewed version available at Polymers 2018, 10, 1304; doi:10.3390/polym10121304

3.4. The impact assessment of filament formation on selected S-TPU properties.

3.4.1. Fourier transform infrared spectroscopy (FTIR)

FTIR spectra of obtained S-TPUs and extruded F-TPU filament was presented in Figure 3. The band assignments with a description were given in Table 3. The interpretation of the particular bands was made on the basis of a Silverstein et. all [54] scientific book. The presence of functional groups characteristic for poly(ester urethane)s was confirmed (Table 3) and the results are consistent with the interpretation given by Yiligor et al. [55]. The FTIR spectra of S-TPU and F-TPU are very similar, which might suggest that extrusion process did not cause any chemical changes in S-TPU structure.

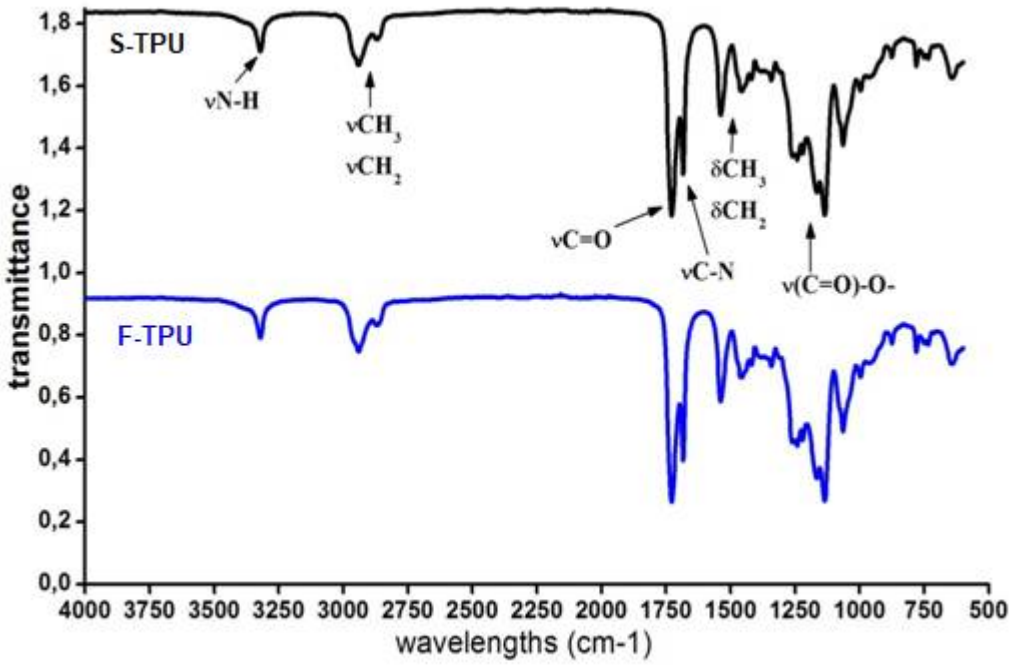

Figure 3. The FTIR spectra of S-TPU and extruded F-TPU filament.

In both spectra, a weak absorption peaks assigned to N–H stretching vibrations are observed at 3324 cm^{-1}, which is related with the presence of hydrogen bonds between NH groups and macrodiol's ester groups (C=O). The peaks, which appeared between 2941 – 2863 cm^{-1} correspond to the asymmetric and symmetric stretching vibrations of aliphatic CH_2 groups presented in S-TPU structure. Strong signals registered in the range of 1733 – 1685 cm^{-1} are related to stretching of C=O (both, hydrogen bonded and not hydrogen bonded in ester groups of macrodiol). Polyurethanes characteristic peak from C–N stretching are seen at 1535 cm^{-1}. Peaks observed at 1465 – 1336 cm^{-1} corresponds to deformation vibrations of aliphatic CH_2 groups present in the S-TPU. Stretching vibrations of –NH-(C=O)-O- (urethane group), were registered at 1165 cm^{-1}. In turn, stretching vibration of hydrogen bonded -C-(C=O)-O-, is presented between 1135 – 947 cm^{-1}. Finally, peaks in the range of 873 – 863 are associated with out of plane bondings vibrations of; C–H bending, CH_2, NH, OH wagging and scissoring. According to physicochemical tables [54], absorbance in the range of 2250 – 2270 cm^{-1} are assigned to free NCO groups. The absence of those peaks indicate the complete reaction between reagents (HDI, PEBA, BDO) until the -NCO groups are completely convert into urethanes functional groups. This is also in accordance with identification of free isocyanate groups during pre-polymerization stage. FTIR analysis confirmed that F-TPU has the same chemical bonding type as bulk S-TPU and the filament formation process did not affect its chemical structure.

Table 1 Band assignments noted at the FTIR spectra of S-TPU and F-TPU filament.

S-TPU	F-TPU	Band	Description
Wavelength (cm^{-1})			
3324 w	3324 w	νNH	stretching of NH groups. These groups were hydrogen bonded with C=O of ester groups present in macrodiol
2941 w, 2863 w	2939 w, 2865 w	νCH_2, νCH_3	stretching of aliphatic asymmetric and symmetric CH_2 groups present in the S-TPU chain and in the S-TPU filament
1730 vs -1686 s	1733 vs – 1685 s	νC=O	stretching of C=O in ester groups of macrodiol, (hydrogen bonded and not hydrogen bonded)
1535 s	1535 s	νC-N	stretching of C-N in urethane group
1459 w - 1336 vw	1465 w - 1346 w	δCH_2	deformation vibrations of aliphatic CH_2 groups present in the S-TPU and S-TPU filament: bending, wagging, scissoring in plane
1259 m - 1219 m	1257 s - 1216 m	νC-(C=O)-O	stretching vibrations of -C-(C=O)-O- (ester group), not hydrogen bonded
1165 s	1165 m	νNH-(C=O)-O	stretching vibrations of –NH-(C=O)-O- of urethane group
1129 s - 994 w	1135 s - 947 m,	νC-(C=O)-O νC-O	stretching vibration of hydrogen bonded -C-(C=O)-O-,
873 w - 642 w	873 w - 638 m	δCH_2, δNH, δOH	out of the plane deformation of CH_2(scissoring/wagging) as well as NH and OH groups (scissoring and wagging).

3.4.2. Optical microscopy (OM)

The optical microscopy of S-TPU and F-TPU filament was presented in Figure 4.

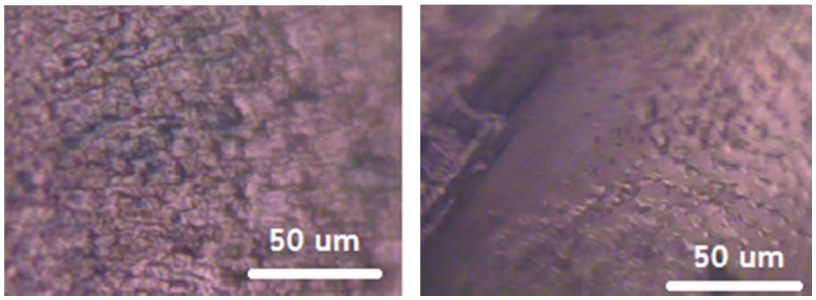

(a) (b)

Figure 1 Optical microscopy of a) bulk S-TPU and b) F-TPU filament.

Surfaces of prepared brittle fractures of S-TPU and extruded F-TPU were very homogenous and characteristic image for un-crosslinked TPUs was observed. No radial structures [56] proper for crosslinked TPU [57] were observed.

3.4.3. Water contact angle (CA)

Water contact angle studies allow to specify the hydrophilicity/hydrophobicity of the material surface. However, CA is not a sufficient indicator to determine the biocompatibility of the material. Notwithstanding, hydrophilicity is an important biomedical parameter that favors the adherence

Peer-reviewed version available at Polymers 2018, 10, 1304; doi:10.3390/polym10121304

and interaction of cells with material surfaces, thus CA studies provide preliminary biomedical characterization [58].

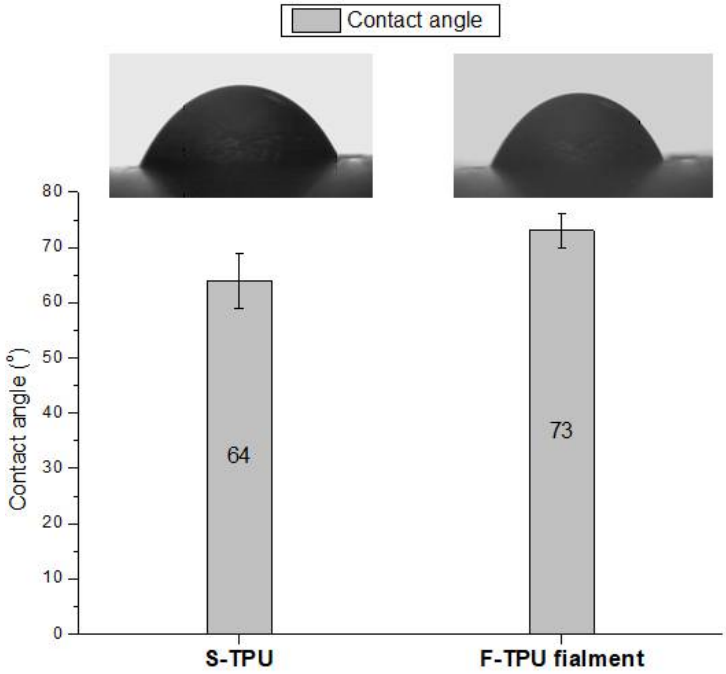

Figure 5. Contact angle of pure S-TPU and of extruded F-TPU filament.

Results of CA measurements of S-TPU and F-TPU were presented in Figure 5. The analysis of CA revealed that the extrusion process slightly increased the CA from 64º for S-TPU to 73º for F-TPU filament. Thus, the material became more hydrophobic after processing, which can be explained by the smoother surface presented by F-TPU filament. However, obtained values are still within the range of 55-75° that ensures proper adhesion of human cells to the surface of the selected material [47].

3.5. Biological studies

3.5.1. Short-term hemocompatibility test.

One of the test methods to evaluate biological properties *in vitro* is study on blood response. Synthetic materials marked as medical-grade are intended for directly or indirectly contact with body tissues, such as blood. Therefore, the study of the interaction of material with blood which is the fluid tissue present in every part of the body, seems to be important. It is a known fact that all of the biomaterials which are in contact with body tissues, cause the initiation of an inflammatory reaction (foreign body response FBR) [59]. Occurrence of acute or chronic reactions for a long time, disqualifies the material in medical applications. An initial interaction of cellular blood components with artificial/synthetic surface occurs after first minutes of contact. Consequently, short-term studies of the interaction material – blood, can provide preliminary information about biocompatibility of the material.

Analysis of the obtained data (Figure 6) showed that both, synthesized S-TPU and extruded F-TPU filament can be pre-classified as biocompatible materials, under the specified conditions. Thus, the extrusion process did not influence this parameter and obtained materials may find a potential applications in blood-contacting medical devices. This is consistent with the references related to the fact that PURs are one of the most hemocompatible synthetic polymers dedicated to the medical applications [60].

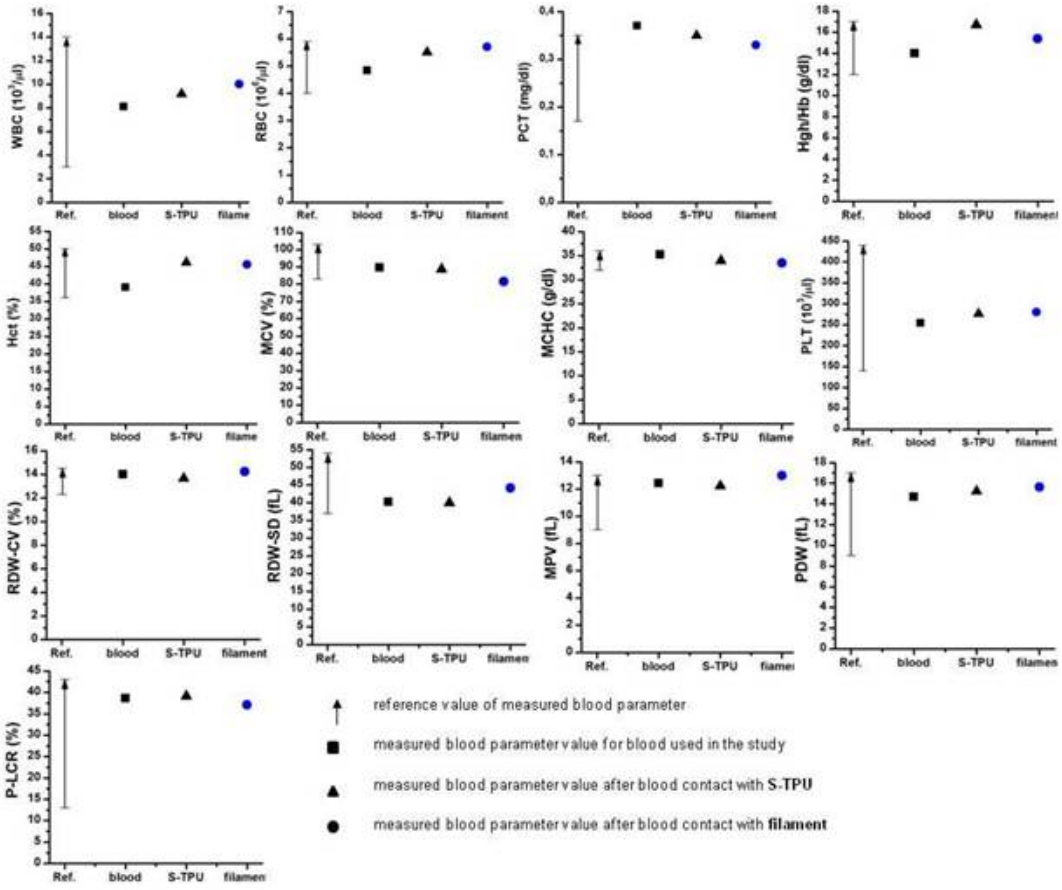

Figure 6. Short-term biocompatibility of S-TPU and extruded F-TPU filament with human blood. WBC - white blood cells (leucocytes); RBC - red blood cells (erythrocytes); PCT - percentage of platelets in whole blood volume; Hgh/Hb - hemoglobin; Hct – hematocrit; MCV mean corpuscular volume; MCHC - mean concentration of hemoglobin in blood cells; PLT - platelet amount (thrombocytes); RDW-CV/RDW-SD - distribution volume of red blood cells; MPV - mean platelet volume; PDW - indicator of platelet volume distribution; P-LCR - platelet larger cell ratio.

It should be noted that, all of the studied blood parameters are in the references range and they do not differ significantly from the values obtained for pure blood. Hemocompatibility test indicated that both S-TPU and F-TPU did not change cell count of; MCV, MCHC, PLT, RDW-CV, RDW-SD, MPV, PDW, P-LCR. On the contrary to WBC, RBC, PCT, Hgh/Hb, Hct, which have changed slightly. A slight decrease in the PCT value corresponding to the platelet count was observed. It can be related to aggregation and activation of platelets on the S-TPU surface [61]. This is an undesirable phenomenon that can lead to thrombosis [62]. Nevertheless, this value is still in the norm. An increase of white blood cells (WBC) number was noticed, which is related to an initial inflammatory reaction that always takes place when in contact with an artificial organism. In turn, blood parameter associated with erythrocytes (RBC, Hgh/Hb, Hct), slightly increase to the maximum reference value, after contact with S-TPU and extruded F-TPU. Eventually, significant reduction in RBC and Hct values could indicate the adhesion to the surfaces of erythrocytes, which in turn have a tendency to aggregate and form the so-called blood cloths [63].

3.5.2. Cytotoxicity

The cytotoxicity of obtained S-TPU and F-TPU filament was shown in Figure 7. As it can be observed, both materials indicated biocompatibility towards NIH 3T3 cells. For S-TPU after 24h and 48h of incubation the proliferation of cells was noted (over 100% of cells viability), while for F-TPU it was 95%, 86% and 79% after 24h, 48h, and 72h, respectively. Slight differences in biocompatibility can be directly related to the higher hydrophilicity of S-TPU surface than extruded F-TPU.

Peer-reviewed version available at Polymers 2018, 10, 1304; doi:10.3390/polym10121304

Moreover, the greater roughness and irregular surface the better adhesion of cells to the substrate, was noted [64], hence the possible difference in cell proliferation in the differentiation to F-TPU filament.

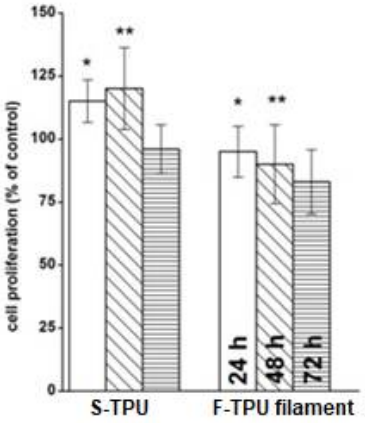

Figure 7. The effect of S-TPU and extruded F-TPU extracts on the in vitro growth of mouse embryonic fibroblast NIH 3T3 cells measured using MTT assay. Cell proliferation is represented as a percentage of control cell growth in cultures containing no S-TPU or extruded S-TPU filament extracts. Results are a mean ± SD of two separate experiments wherein each treatment condition was repeated in two wells. * $p < 0.05$; ** $p < 0.001$ vs. control.

Morphology of cells was observed for 72h and the images were presented in Figure 8. As it can be seen, S-TPU and F-TPU filament extracts did not significantly change the morphology of the NIH 3T3 cells.

	Control	S-TPU	F-TPU filament
24 h	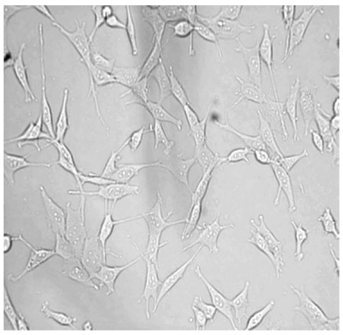	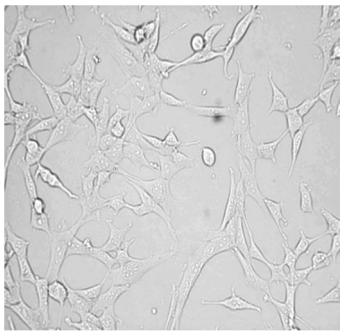	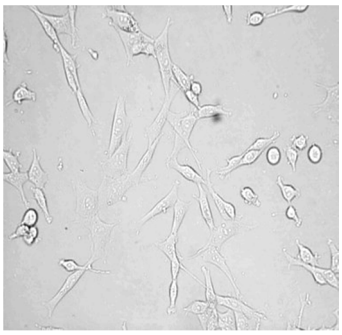
48 h	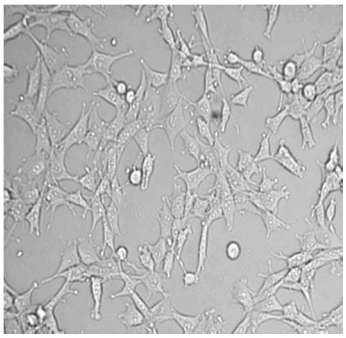	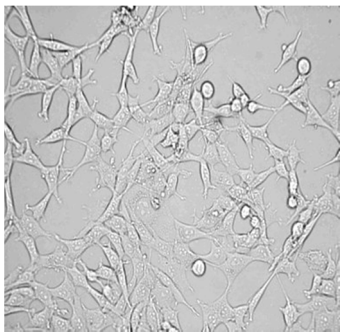	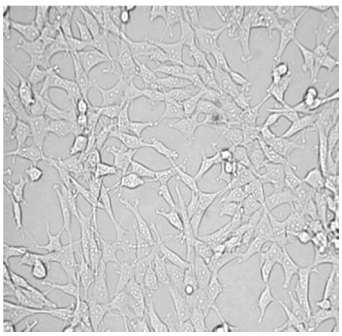

Peer-reviewed version available at Polymers 2018, 10, 1304; doi:10.3390/polym10121304

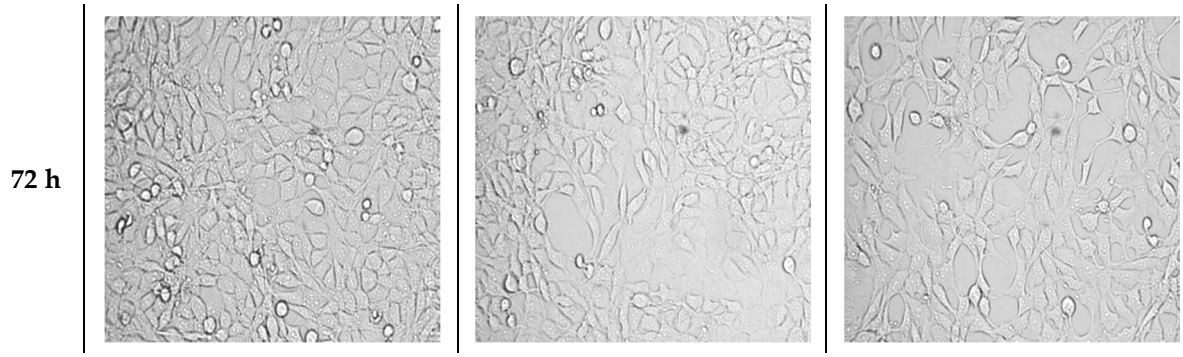

Figure 8. The effect of S-TPU and F-TPU filament extracts on the cellular morphology of mouse embryonic fibroblast NIH 3T3 cells.

The morphology of NIH 3T3 cells did not changed and was comparable to the control up to 72h of incubation. Shape and cells dimensions were not impaired. It should be noted that, there was a slight decrease in cells number when they had contact with F-TPU filament, in comparison to the control sample. However, no cells degeneration or apoptosis was noticed during the incubation both S-TPU and F-TPU. This might be explained by hindered cell adhesion to the F-TPU substrate, which exhibits higher contact angle and smother surface than bulk S-TPU. Thus, these materials may be considered as a suitable for biomedical applications.

4. Conclusions

In this work we reported the synthesis, processing, physico-mechanical characterization and biological studies of new uncatalyzed aliphatic, amorphous, polyurethane, as a potential medical-grade filament for using in FDM 3D printing technology.

For these purpose, bulk S-TPU with 1,1:1 NCO:OH molar ratio was synthesized and the efforts have been made to adjust the temperature profile and operating parameters of S-TPU melt-extrusion. Established extrusion processing temperature for S-TPU was in the range of 160 - 205 ºC, respectively. As a result a stable F-TPU filament with 1,75 mm diameter was received. The mechanical characteristic and MFR of S-TPU is satisfactory which has references to FDM 3D printing, where the ease of processing, stability in print conditions and the proper flow, viscosity and hardness of the filament are responsible for the print quality. The summary of the obtained S-TPU mechanical properties and its comparison to the commercial medical-grade PURs in terms of mechanical efficiency was given in Table 4.

Table 2 Comparison of available medical-grade polyurethanes properties with synthesized uncatalyzed S-TPU system. (The data were taken from the material safety data sheets available on manufacturers' websites).

Value range	MilaMed®	Desmopan® AU	Texin®RxT50	S-TPU
TSb [MPa]	15-30	25-50	25-52	26
Eb [%]	540-565	470-880	320-770	705
HS [ºSh A/D]	no data found	60A - 75D	70A - 65D	26D
Chemical composition	Aliphatic polyether	Aromatic polyester	Aromatic polyether	Aliphatic polyester

It can be seen that the mechanical properties of synthesized S-TPU are within the range of values suitable for medical-grade polyurethanes such as; MillaMed®, Desmopan® or Texin®. Thus, obtained uncatalysed aliphatic S-TPUs seem to be a promising candidate as a filament material for FDM 3D printer for medical purpose. Preliminary biological studies showed biocompatibility and hemocompatibility of F-TPU filament and provided that, this material may find application as a novel medical-grade, flexible filament for FDM 3DP. To confirm the validity of the presented studies, a test print of anatomical flexible heart using F-TPU filament and FDM type 3D printer, was

made. Results are presented in **supplementary data 2**. The initial evaluation of FDM print with the use of obtained F-TPU filament allows to conclude that obtained F-TPU filament is suitable for 3D printing in the FDM type technology. Fabrication of F-TPU filament combined with 3DP technology allows for fabrication of customized and repeatable products without the use of toxic substances during printing. Moreover, the 3D printing technology in combination with elastomeric filament let to design cost-efficient and achievable patient - customized products.

Supplementary Materials. The following are available online at www.mdpi.com/xxx/s1. Supplementary data 1 provides the results and methodology of accelerated degradation studies on Bioflex® and F-TPU filaments as well microscopic analysis of degraded samples. Supplementary data 2 presents trial of FDM 3D printing process using obtained F-TPU filament.

Author Contributions: Writing-original draft and Investigation A.H., Writing-review & editing, I.G., Funding and Supervision, J.K-L., H.J.

Acknowledgments: The work was supported by the Gdansk University of Technology, Narutowicza St. 11/12, 80-233 Gdansk, Poland.

Conflicts of Interest: The authors declare no conflict of interest.

References

1. Javaid, M.; Haleem, A. Additive manufacturing applications in medical cases: A literature based review. *Alexandria J. Med.* **2017**, doi:10.1016/j.ajme.2017.09.003.

2. Schubert, C.; Van Langeveld, M. C.; Donoso, L. A. Innovations in 3D printing: A 3D overview from optics to organs. *Br. J. Ophthalmol.* **2014**, *98*, 159–161, doi:10.1136/bjophthalmol-2013-304446.

3. Ventola, C. L. Medical Applications for 3D Printing: Current and Projected Uses. *Pharm. Ther.* **2014**, *39*, 704–711, doi:10.1016/j.infsof.2008.09.005.

4. Klammert, U.; Gbureck, U.; Vorndran, E.; Rödiger, J.; Meyer-Marcotty, P.; Kübler, A. C. 3D powder printed calcium phosphate implants for reconstruction of cranial and maxillofacial defects. *J. Cranio-Maxillofacial Surg.* **2010**, *38*, 565–570, doi:10.1016/j.jcms.2010.01.009.

5. Bergmann, C.; Lindner, M.; Zhang, W.; Koczur, K.; Kirsten, A.; Telle, R.; Fischer, H. 3D printing of bone substitute implants using calcium phosphate and bioactive glasses. *J. Eur. Ceram. Soc.* **2010**, *30*, 2563–2567, doi:10.1016/j.jeurceramsoc.2010.04.037.

6. Lee, M.-Y.; Chang, C.-C.; Ku, Y. C. New layer-based imaging and rapid prototyping techniques for computer-aided design and manufacture of custom dental restoration. *J. Med. Eng. Technol.* **2008**, *32*, 83–90, doi:10.1080/03091900600836642.

7. O 'reilly, M. K.; Reese, S.; Herlihy, T.; Geoghegan, T.; Cantwell, C. P.; Feeney, R. N. M.; Jones, J. F. X. Fabrication and Assessment of 3D Printed Anatomical Models of the Lower Limb for Anatomical Teaching and Femoral Vessel Access Training in Medicine., doi:10.1002/ase.1538.

8. Qiu, K.; Zhao, Z.; Haghiashtiani, G.; Guo, S.-Z.; He, M.; Su, R.; Zhu, Z.; Bhuiyan, D. B.; Murugan, P.; Meng, F.; Park, S. H.; Chu, C.-C.; Ogle, B. M.; Saltzman, D. A.; Konety, B. R.; Sweet, R. M.; McAlpine, M. C. 3D Printed Organ Models with Physical Properties of Tissue

and Integrated Sensors. *Adv. Mater. Technol.* **2017**, *1700235*, 1–9, doi:10.1002/admt.201700235.

9. Garcia, J.; Yang, Z.; Mongrain, R.; Leask, R. L.; Lachapelle, K. 3D printing materials and their use in medical education: a review of current technology and trends for the future. *BMJ Simul. Technol. Enhanc. Learn.* **2017**, bmjstel-2017-000234, doi:10.1136/bmjstel-2017-000234.

10. Ikada, Y. Challenges in tissue engineering. *J. R. Soc. Interface* **2006**, *3*, 589–601, doi:10.1098/rsif.2006.0124.

11. Hutmacher, D. W. Scaffolds in tissue engineering bone and cartilage. *Biomaterials* **2000**, *21*, 2529–43.

12. ASTM F2792-10, Standard Terminology for Additive Manufacturing Technologies, ASTM International, West Conshohocken, PA, 2010.

13. Kim, G. B.; Lee, S.; Kim, H.; Yang, D. H.; Kim, Y.-H.; Kyung, Y. S.; Kim, C.-S.; Choi, S. H.; Kim, B. J.; Ha, H.; Kwon, S. U.; Kim, N. Three-Dimensional Printing: Basic Principles and Applications in Medicine and Radiology. *Korean J. Radiol.* **2016**, *17*, 182–97, doi:10.3348/kjr.2016.17.2.182.

14. Monti, M. Bioprinting in Regenerative Medicine. *Eur. J. Histochem.* **2016**, *60*, doi:10.4081/ejh.2016.2627.

15. Bartolo, P.; Domingos, M.; Gloria, A.; Ciurana, J. BioCell Printing: Integrated automated assembly system for tissue engineering constructs. *CIRP Ann. - Manuf. Technol.* **2011**, *60*, 271–274, doi:10.1016/j.cirp.2011.03.116.

16. Oskui, S. M.; Diamante, G.; Liao, C.; Shi, W.; Gan, J.; Schlenk, D.; Grover, W. H. Assessing and Reducing the Toxicity of 3D-Printed Parts. *Environ. Sci. Technol. Lett.* **2016**, *3*, 1–6, doi:10.1021/acs.estlett.5b00249.

17. Xu, N.; Ye, X.; Wei, D.; Zhong, J.; Chen, Y.; Xu, G.; He, D. 3D artificial bones for bone repair prepared by computed tomography-guided fused deposition modeling for bone repair. *ACS Appl. Mater. Interfaces* **2014**, *6*, 14952–14963, doi:10.1021/am502716t.

18. Vargas-Alfredo, N.; Dorronsoro, A.; Cortajarena, A. L.; Rodríguez-Hernández, J. Antimicrobial 3D Porous Scaffolds Prepared by Additive Manufacturing and Breath Figures. *ACS Appl. Mater. Interfaces* **2017**, *9*, 37454–37462, doi:10.1021/acsami.7b11947.

19. Melocchi, A.; Parietti, F.; Maroni, A.; Foppoli, A.; Gazzaniga, A.; Zema, L. Hot-melt extruded filaments based on pharmaceutical grade polymers for 3D printing by fused deposition modeling. *Int. J. Pharm.* **2016**, *509*, 255–263, doi:10.1016/j.ijpharm.2016.05.036.

20. Mohseni, M.; Hutmacher, D. W.; Castro, N. J. Independent evaluation of medical-grade bioresorbable filaments for fused deposition modelling/fused filament fabrication of tissue engineered constructs. *Polymers (Basel).* **2018**, *10*, doi:10.3390/polym10010040.

21. O'Brien, F. J. Biomaterials & scaffolds for tissue engineering. *Mater. Today* **2011**, *14*, 88–95, doi:10.1016/S1369-7021(11)70058-X.

22. Patrício, T.; Domingos, M.; Gloria, A.; Bártolo, P. Characterisation of PCL and PCL/PLA scaffolds for tissue engineering. *Procedia CIRP* **2013**, *5*, 110–114, doi:10.1016/j.procir.2013.01.022.

23. Zein, I.; Hutmacher, D. W.; Tan, K. C.; Teoh, S. H. Fused deposition modeling of novel scaffold architectures for tissue engineering applications. *Biomaterials* **2002**, *23*, 1169–85.

24. Hutmacher, D. W.; Schantz, T.; Zein, I.; Ng, K. W.; Teoh, S. H.; Tan, K. C. Mechanical properties and cell cultural response of polycaprolactone scaffolds designed and fabricated via fused deposition modeling. *J. Biomed. Mater. Res.* **2001**, *55*, 203–216, doi:10.1002/1097-4636(200105)55:2<203::AID-JBM1007>3.0.CO;2-7.

25. Kucinska-Lipka, J.; Gubanska, I.; Strankowski, M.; Cieśliński, H.; Filipowicz, N.; Janik, H. Synthesis and characterization of cycloaliphatic hydrophilic polyurethanes, modified with L-ascorbic acid, as materials for soft tissue regeneration. *Mater. Sci. Eng. C* **2017**, *75*, 671–681, doi:10.1016/j.msec.2017.02.052.

26. Cauich-rodríguez, J. V; Chan-Chan, L. H.; Hernandez-Sánchez, F.; Cervantes-Uc, J. M. Degradation of Polyurethanes for Cardiovascular Applications. In *Advances in Biomaterials Science and Biomedical Applications*; Pignatello, R., Ed.; InTech, 2012; pp. 51–82 ISBN 978-953-51-1051-4.

27. Davis, F. J.; Mitchell, G. R. Polyurethane Based Materials with Applications in Medical Devices. In *Bio-Materials and Prototyping Applications in Medicine*; CRC press: Washington, DC, 2008; pp. 27–48.

28. Kucińska-Lipka, J.; Gubanska, I.; Pokrywczynska, M.; Ciesliński, H.; Filipowicz, N.; Drewa, T.; Janik, H. Polyurethane porous scaffolds (PPS) for soft tissue regenerative medicine applications. *Polym. Bull.* **2017**, 1–23, doi:10.1007/s00289-017-2124-x.

29. Borkenhagen, M.; Stoll, R. C.; Neuenschwander, P.; Suter, U. W.; Aebischer, P. In vivo performance of a new biodegradable polyester urethane system used as a nerve guidance channel. *Biomaterials* **1998**, *19*, 2155–65.

30. Lamba, N. M. K.; Woodhouse, K. A.; Cooper, S. L.; Lelah, M. D. *Polyurethanes in biomedical applications*; CRC press: Washington, DC, 1998; ISBN 9780849345173.

31. Jung, S. Y.; Lee, S. J.; Kim, H. Y.; Park, H. S.; Wang, Z.; Kim, H. J.; Yoo, J. J.; Chung, S. M.; Kim, H. S. 3D printed polyurethane prosthesis for partial tracheal reconstruction: a pilot animal study. *Biofabrication* **2016**, *8*, 045015, doi:10.1088/1758-5090/8/4/045015.

32. Tsai, K. J.; Dixon, S.; Hale, L. R.; Darbyshire, A.; Martin, D.; de Mel, A. Biomimetic heterogenous elastic tissue development. *npj Regen. Med.* **2017**, *2*, 16,

536 doi:10.1038/s41536-017-0021-4.

537 33. Kucińska-Lipka, J.; Gubanska, I.; Skwarska, A. Microporous Polyurethane Thin Layer as a
538 Promising Scaffold for Tissue Engineering. *Polymers (Basel).* **2017**, *9*, 277,
539 doi:10.3390/polym9070277.

540 34. Park, H.; Gong, M.-S.; Knowles, J. C. Catalyst-free synthesis of high elongation degradable
541 polyurethanes containing varying ratios of isosorbide and polycaprolactone: physical
542 properties and biocompatibility. *J. Mater. Sci. Mater. Med.* **2013**, *24*, 281–294,
543 doi:10.1007/s10856-012-4814-0.

544 35. Kim, H.-J.; Kang, M.-S.; Knowles, J. C.; Gong, M.-S. Synthesis of highly elastic biocompatible
545 polyurethanes based on bio-based isosorbide and poly(tetramethylene glycol) and their
546 properties. *J. Biomater. Appl.* **2014**, *29*, 454–464, doi:10.1177/0885328214533737.

547 36. Tanzi, M. C.; Verderio, P.; Lampugnani, M. G.; Resnati, M.; Dejana, E.; Sturani, E.
548 Cytotoxicity of some catalysts commonly used in the synthesis of copolymers for biomedical
549 use. *J. Mater. Sci. Mater. Med.* **1994**, *5*, 393–396, doi:10.1007/BF00058971.

550 37. Hassan, M.; Mauritz, K.; Storey, R.; Wiggins, J. Biodegradable Aliphatic Thermoplastic
551 Polyurethane Based on Poly(e-caprolactone) and L-Lysine Diisocyanate. *J. Polym. Sci. Part A*
552 *Polym. Chem.* **2006**, *44*, 2990–3000, doi:10.1002/pola.21373.

553 38. Heijkants, R. G. J. C.; Van Calck, R. V.; Van Tienen, T. G.; De Groot, J. H.; Buma, P.; Pennings,
554 A. J.; Veth, R. P. H.; Schouten, A. J. Uncatalyzed synthesis, thermal and mechanical properties
555 of polyurethanes based on poly(ε-caprolactone) and 1,4-butane diisocyanate with uniform
556 hard segment. *Biomaterials* **2005**, *26*, 4219–4228, doi:10.1016/j.biomaterials.2004.11.005.

557 39. Barrioni, B. R.; De Carvalho, S. M.; Oréfice, R. L.; De Oliveira, A. A. R.; Pereira, M. D. M.
558 Synthesis and characterization of biodegradable polyurethane films based on HDI with
559 hydrolyzable crosslinked bonds and a homogeneous structure for biomedical applications.
560 *Mater. Sci. Eng. C* **2015**, *52*, 22–30, doi:10.1016/j.msec.2015.03.027.

561 40. Janik, H. Z. Struktury nadcząsteczkowe i wybrane właściwości rozgałęzionych i
562 usieciowanych poli(estro-uretanów), poli(etero-uretanów) i poli(uretano-biuretów)
563 formowanych reaktywnie. *Zesz. Nauk. Politech. Gdańskiej. Chem.* **2005**, *Nr 53(599)*, 3–141.

564 41. Pietrzak, K.; Isreb, A.; Alhnan, M. A. A flexible-dose dispenser for immediate and extended
565 release 3D printed tablets. *Eur. J. Pharm. Biopharm.* **2015**, *96*, 380–387,
566 doi:10.1016/j.ejpb.2015.07.027.

567 42. Sun, Q.; Rizvi, G. M.; Bellehumeur, C. T.; Gu, P. Effect of processing conditions on the
568 bonding quality of FDM polymer filaments. *Rapid Prototyp. J.* **2008**, *14*, 72–80,
569 doi:10.1108/13552540810862028.

570 43. Gkartzou, E.; Koumoulos, E. P.; Charitidis, C. A. Production and 3D printing processing of

bio-based thermoplastic filament. *Manuf. Rev.* **2017**, *4*, 1, doi:10.1051/mfreview/2016020.

44. Nezarati, R. M.; Eifert, M. B.; Dempsey, D. K.; Cosgriff-Hernandez, E. Electrospun vascular grafts with improved compliance matching to native vessels. *J. Biomed. Mater. Res. Part B Appl. Biomater.* **2015**, *103*, 313–323, doi:10.1002/jbm.b.33201.

45. Qin, Y.; Liu, R.; Zhao, Y.; Hu, Z.; Li, X. Preparation of Dipyridamole/Polyurethane Core–Shell Nanofibers by Coaxial Electrospinning for Controlled-Release Antiplatelet Application. *J. Nanosci. Nanotechnol.* **2016**, *16*, 6860–6866, doi:10.1166/jnn.2016.11386.

46. Wang, H.; Feng, Y.; Fang, Z.; Yuan, W.; Khan, M. Co-electrospun blends of PU and PEG as potential biocompatible scaffolds for small-diameter vascular tissue engineering. *Mater. Sci. Eng. C* **2012**, *32*, 2306–2315, doi:10.1016/j.msec.2012.07.001.

47. Wang, H.; Feng, Y.; An, B.; Zhang, W.; Sun, M.; Fang, Z.; Yuan, W.; Khan, M. Fabrication of PU/PEGMA crosslinked hybrid scaffolds by in situ UV photopolymerization favoring human endothelial cells growth for vascular tissue engineering. *J. Mater. Sci. Mater. Med.* **2012**, *23*, 1499–1510, doi:10.1007/s10856-012-4613-7.

48. Yuan, W.; Feng, Y.; Wang, H.; Yang, D.; An, B.; Zhang, W.; Khan, M.; Guo, J. Hemocompatible surface of electrospun nanofibrous scaffolds by ATRP modification. *Mater. Sci. Eng. C* **2013**, *33*, 3644–3651, doi:10.1016/j.msec.2013.04.048.

49. NinjaTek Technical Sepcification of NinjaFlex 3D Printing Filament Available online: https://ninjatek.com/wp-content/uploads/2016/05/NinjaFlex-TDS.pdf (accessed on Mar 4, 2018).

50. Chen, R.; Huang, C.; Ke, Q.; He, C.; Wang, H.; Mo, X. Preparation and characterization of coaxial electrospun thermoplastic polyurethane/collagen compound nanofibers for tissue engineering applications. *Colloids Surfaces B Biointerfaces* **2010**, *79*, 315–325, doi:10.1016/j.colsurfb.2010.03.043.

51. Detta, N.; Errico, C.; Dinucci, D.; Puppi, D.; Clarke, D. A.; Reilly, G. C.; Chiellini, F. Novel electrospun polyurethane/gelatin composite meshes for vascular grafts. *J. Mater. Sci. Mater. Med.* **2010**, *21*, 1761–1769, doi:10.1007/s10856-010-4006-8.

52. Filoalfa - Bioflex filament Available online: https://www.filoalfa3d.com/en/filaments-175mm/296-bioflex-pla-shore-27d-white-o-175-mm-8050327032385.html (accessed on Mar 4, 2018).

53. Kucinska-Lipka, J.; Gubanska, I.; Sienkiewicz, M. Thermal and mechanical properties of polyurethanes modified with L-ascorbic acid. *J. Therm. Anal. Calorim.* **2017**, *127*, 1631–1638, doi:10.1007/s10973-016-5743-9.

54. Socrates, G. *Infrared and Raman Characteristic Group Frequencies: Tables and Charts*; third.; John Wiley & Sons, Ltd., 2004; ISBN 978-0-470-09307-8.

606 55. Yilgor, I.; Yilgor, E.; Guler, I. G.; Ward, T. C.; Wilkes, G. L. FTIR investigation of the influence
607 of diisocyanate symmetry on the morphology development in model segmented
608 polyurethanes. *Polymer (Guildf).* **2006**, *47*, 4105–4114, doi:10.1016/j.polymer.2006.02.027.

609 56. Janik, H. Progress in the studies of the supermolecular structure of segmented polyurethanes.
610 *Polimery* **2010**, *55*, 419–500.

611 57. Kucińska-Lipka, J.; Janik, H.; Balas, A. SYNTHESES, CHEMICAL STRUSTURES AND
612 PROPERTIES OF POLY(ESTER-ETHERURE- THANE)S CROSSLINKED WITH STYRENE,
613 SYNTHESIZED FROM UNSATURATED OLIGO(AL- KYLENE ESTER-ETHER)DIOLS AND
614 4,4'-DIPHENYLMETHANE DIISOCYANATE. *Polimery/Polymers* **2009**, *54*, 781–785.

615 58. Menzies, K. L.; Jones, L. The impact of contact angle on the biocompatibility of biomaterials.
616 *Optom. Vis. Sci.* **2010**, *87*, 387–399, doi:10.1097/OPX.0b013e3181da863e.

617 59. Anderson, J.; Rodrigues, A.; Chang, D. Ferogin Body Reaction To Biometerials. *Semin.*
618 *Immunol.* **2008**, *20*, 86–100, doi:10.1016/j.smim.2007.11.004.

619 60. Fromstein, J. D.; Woodhouse, K. A. Elastomeric biodegradable polyurethane blends for soft
620 tissue applications. *J. Biomater. Sci. Polym. Ed.* **2002**, *13*, 391–406,
621 doi:10.1163/156856202320253929.

622 61. Xin, Z.; Du, B.; Wang, Y.; Qian, S.; Li, W.; Gao, Y.; Sun, M.; Luan, S.; Yin, J.
623 Hemocompatibility Evaluation of Polyurethane Film with Surface-Grafted Sugar- Based
624 Amphipathic Compounds. *J. Anal. Bioanal. Tech.* **2017**, *8*, 1–6, doi:10.4172/2155-9872.1000357.

625 62. Williams, D. F. On the mechanisms of biocompatibility. *Biomaterials* **2008**, *29*, 2941–2953,
626 doi:10.1016/j.biomaterials.2008.04.023.

627 63. Tahara, D.; Oikawa, N.; Kurita, R. Mobility enhancement of red blood cells with biopolymers.
628 *J. Phys. Soc. Japan* **2016**, *85*, 10–12, doi:10.7566/JPSJ.85.033801.

629 64. Keshel, S. H.; Azhdadi, S. N. K.; Asefnejad, A.; Sadraeian, M.; Montazeri, M.; Biazar, E. The
630 relationship between cellular adhesion and surface roughness for polyurethane modified by
631 microwave plasma radiation. *Int. J. Nanomedicine* **2011**, *6*, 641–647, doi:10.2147/IJN.S17180.

632